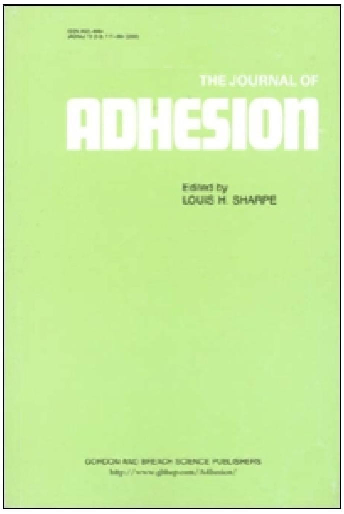

The Journal of Adhesion
Publication details, including instructions for authors and subscription information:
http://www.informaworld.com/smpp/title~content=t713453635

DETERMINATION OF SOLID SURFACE TENSION FROM CONTACT ANGLES: THE ROLE OF SHAPE AND SIZE OF LIQUID MOLECULES

H. Tavana[a]; R. Gitiafroz[a]; M. L. Hair[a]; A. W. Neumann[a]
[a] Department of Mechanical and Industrial Engineering University of Toronto, Toronto, Ontario, Canada

To cite this Article Tavana, H. , Gitiafroz, R. , Hair, M. L. and Neumann, A. W.(2004) 'DETERMINATION OF SOLID SURFACE TENSION FROM CONTACT ANGLES: THE ROLE OF SHAPE AND SIZE OF LIQUID MOLECULES', The Journal of Adhesion, 80: 8, 705 — 725

To link to this Article: DOI: 10.1080/00218460490477675

URL: http://dx.doi.org/10.1080/00218460490477675

The Journal of Adhesion, 80: 705–725, 2004
Copyright © Taylor & Francis Inc.
ISSN: 0021-8464 print/1545-5823 online
DOI: 10.1080/00218460490477675

Taylor & Francis
Taylor & Francis Group

DETERMINATION OF SOLID SURFACE TENSION FROM CONTACT ANGLES: THE ROLE OF SHAPE AND SIZE OF LIQUID MOLECULES

H. Tavana
R. Gitiafroz
M. L. Hair
A. W. Neumann
Department of Mechanical and Industrial Engineering,
University of Toronto, Toronto, Ontario, Canada

Accurate surface tension of Teflon® AF 1600 was determined using contact angles of liquids with bulky molecules. For one group of liquids, the contact angle data fall quite perfectly on a smooth curve corresponding to $\gamma_{sv} = 13.61\,mJ/m^2$, with a mean deviation of only ± 0.24 degrees from this curve. Results suggest that these liquids do not interact with the solid in a specific fashion. However, contact angles of a second group of liquids with fairly bulky molecules containing oxygen atoms, nitrogen atoms, or both deviate somewhat from this curve, up to approximately 3 degrees. Specific interactions between solid and liquid molecules and reorientation of liquid molecules in the close vicinity of the solid surface are the most likely causes of the deviations. It is speculated that such processes induce a change in the solid–liquid interfacial tension, causing the contact angle deviations mentioned above. Criteria are established for determination of accurate solid surface tensions.

Keywords: Liquids with bulky molecules; Surface tension; Contact angle deviations; Teflon® AF 1600; Electronegativity; ADSA-P

Received 16 February 2004; in final form 23 March 2004.

One of a collection of papers honoring A. W. Neumann, the recipient in February 2004 of *The Adhesion Society Award for Excellent in Adhesion Science*, *Sponsored by 3M*.

This work was supported by the Natural Science and Engineering Research Council (NSERC) of Canada under grant no. 8278.

Address correspondence to A. W. Neumann, Department of Mechanical and Industrial Engineering, University of Toronto, 5 King's College Road, Toronto, Ontario, Canada M5S 3G8. E-mail: neumann@mie.utoronto.ca

INTRODUCTION

Solid surface tensions are thermodynamic quantities that play important roles in a wide range of industrial applications. Because of immobility of molecules in a solid phase, direct measurement of solid surface tensions is not possible. Thus, several theoretical and experimental approaches have been developed to estimate surface tensions of solids. They include contact angle measurements for different liquids [1–7], direct-force measurements [8–14], solidification front techniques [15–21], film floatation [22–25], sedimentation techniques [26–29], gradient theory [30–32], Lifshitz theory of van der Waals forces [32–35], and theory of molecular interactions [36–39]. Among these approaches, it is believed that contact angles provide the most broadly applicable venue.

Estimating solid-surface tensions from contact angles is based on a relation first recognized by Young [40]. In principle, the contact angle of a liquid drop on a solid surface is determined by the mechanical equilibrium under the action of three interfacial tensions, *i.e.*, the liquid–vapor surface tension, γ_{lv}, the solid–vapor surface tension, γ_{sv}, and the solid–liquid interfacial tension, γ_{sl} (see Figure 1). This equilibrium relation is known as the Young equation:

$$\gamma_{\mathrm{lv}} \cos\theta = \gamma_{\mathrm{sv}} - \gamma_{\mathrm{sl}}, \tag{1}$$

where θ is the Young contact angle. It has been shown that experimental contact angles might not be compatible with the Young equation and, then, should be excluded from interpretation in terms of energetics of solid surfaces. Examples are dissolution of a polymeric surface by the testing liquid during contact angle measurement,

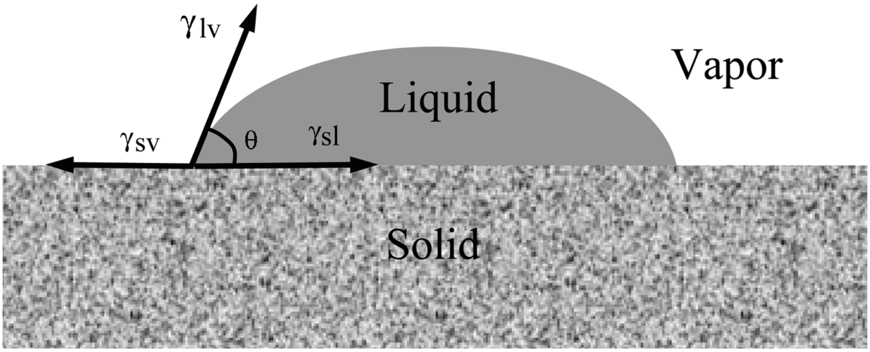

FIGURE 1 Schematic of a sessile drop, contact angle, and the three interfacial tensions.

systems showing slip-stick of the three-phase line, and time-dependent contact angles [41].

The only measurable quantities in the Young equation are γ_{lv} and θ. Therefore, additional information is required. A number of attempts have been made in the literature to determine solid surface tensions from contact angles through Young's equation [1–7]. Although these approaches share similar basic assumptions, their outcomes are in considerable disagreement [41].

By performing contact angle measurements with liquids of different molecular properties on inert polymeric surfaces, it was shown that on one and the same solid surface, $\gamma_{\mathrm{lv}} \cos\theta$ change fairly smoothly and systematically with the liquid surface tension, γ_{lv}. Changing the solid surface shifts the curve in a regular manner [42]. Figure 2 shows typical curves of this type. This implies that

$$\gamma_{\mathrm{lv}} \cos\theta = f(\gamma_{\mathrm{lv}}, \gamma_{\mathrm{sv}}). \tag{2}$$

Combining this relation with the Young equation yields

$$\gamma_{\mathrm{sl}} = F(\gamma_{\mathrm{lv}}, \gamma_{\mathrm{sv}}). \tag{3}$$

This conceptual relation conforms to several equations of state for interfacial tensions in the literature. A well-known example is the geometric-mean combining rule, as first suggested by Berthelot, which when applied to interfacial tensions yields

$$\gamma_{\mathrm{sl}} = \gamma_{\mathrm{lv}} + \gamma_{\mathrm{sv}} - 2\sqrt{\gamma_{\mathrm{lv}}\gamma_{\mathrm{sv}}}. \tag{4}$$

However,this equation is applicable only when $\gamma_{\mathrm{lv}} \approx \gamma_{\mathrm{sv}}$, otherwise the $\sqrt{\gamma_{\mathrm{lv}}\gamma_{\mathrm{sv}}}$ term turns out to be too large. Therefore, a modified combining rule was introduced [4] in the form

$$\gamma_{\mathrm{sl}} = \gamma_{\mathrm{lv}} + \gamma_{\mathrm{sv}} - 2\sqrt{\gamma_{\mathrm{lv}}\gamma_{\mathrm{sv}}}\, e^{-\beta(\gamma_{\mathrm{lv}}-\gamma_{\mathrm{sv}})^2}, \tag{5}$$

where β is a positive constant such that the square root term is appropriately corrected as the two phases become more and more dissimilar.

When $\gamma_{\mathrm{lv}} = \gamma_{\mathrm{sv}}$, this equation reduces to the Berthelot rule because the exponential term becomes unity. Combining Equation (5) with Young's equation yields

$$\cos\theta = -1 + 2\sqrt{\frac{\gamma_{\mathrm{sv}}}{\gamma_{\mathrm{lv}}}}\, e^{-\beta(\gamma_{\mathrm{lv}}-\gamma_{\mathrm{sv}})^2} \tag{6}$$

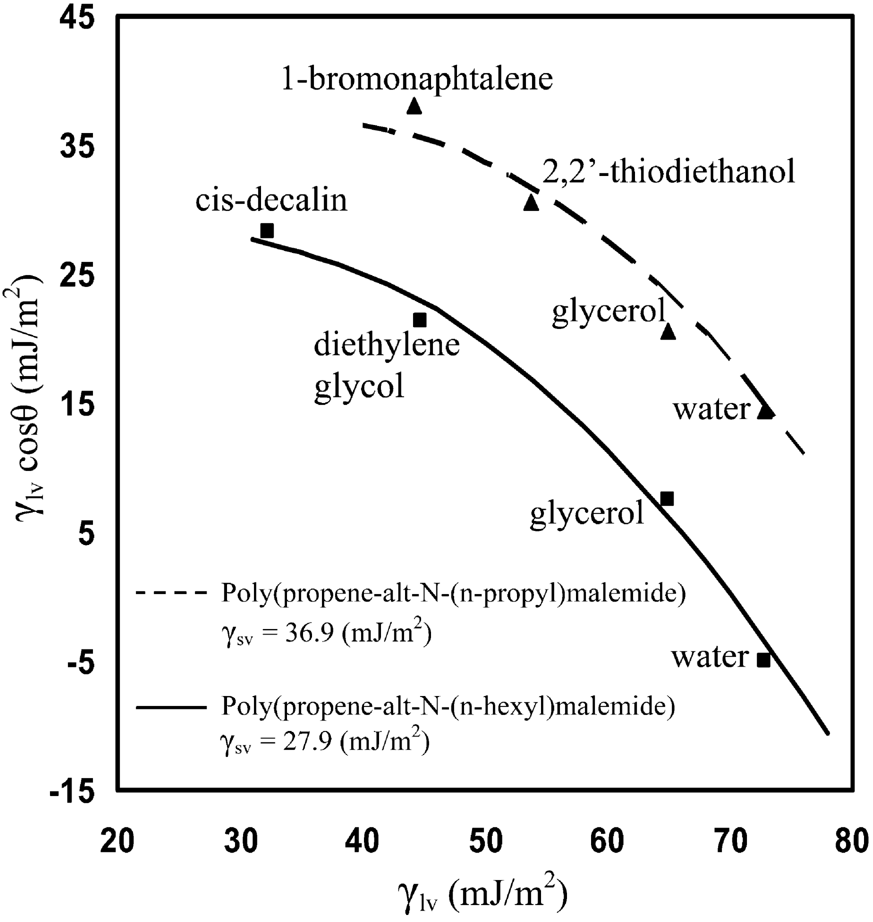

FIGURE 2 Plot of $\gamma_{lv}\cos\theta$ *versus* γ_{lv} for a number of liquids on two polymeric surfaces. The smoothness of the curves implies that $\gamma_{lv}\cos\theta$ is only a function of γ_{lv} and γ_{sv}. Deviations in contact angles from smooth curves are apparent.

This equation contains the two measurable quantities, γ_{lv} and θ; the solid surface tension, γ_{sv}; and the as-yet unknown constant, β. Since we will have, for one and the same solid, a number of experimentally determined pairs of γ_{lv} and θ, obtaining γ_{sv} is then a straightforward matter. Assuming constancy of the γ_{sv} and β values for the array of γ_{lv} and θ pairs, a multivariable optimization scheme can be applied to determine β and γ_{sv} values that provide the best fit of Equation (6) to the experimental pairs of γ_{lv} and θ values for that solid [42]. From contact angle results on fifteen different polymeric surfaces, β was found to have an average value of 0.0001247 ± 0.00001 $(\mathrm{mJ/m^2})^{-2}$ [41]. This narrow error limit implies that the β value is independent of the solid surfaces used for contact angle measurements.

However, close scrutiny of the curves of the type illustrated in Figure 2 shows that even well-measured contact angles do not fall perfectly on the smooth curves. There has always been typical scatter of approximately 1–3 degrees in contact angle data around the curves, which was noted and tentatively attributed to a variety of possible causes. Nevertheless, this scatter introduces an element of uncertainty into the conclusions.

This problem was addressed in an earlier study [43]. Reproducing contact angles of a series of n-alkanes by different operators at different times indicated that the above deviations are not simply experimental errors but must have physical causes. It was shown that contact angles of a group of liquids with bulky molecules on Teflon AF 1600 films fall perfectly on a smooth curve corresponding to $\beta = 0.0001135$ $(\mathrm{mJ/m^2})^{-2}$ and $\gamma_{\mathrm{sv}} = 13.64$ $(\mathrm{mJ/m^2})$, with an average deviation of only ± 0.3 degrees from this curve. That group consisted of cis-decalin, methyl salicylate, octamethylcyclotetrasiloxane (OMCTS), tetralin, and octamethyltrisiloxane (OMTS). The observed pattern suggested that these liquids do not show specific interactions with the solid surface. This results from the bulky shape and inflexible nature of the molecules of these liquids. It appeared that liquids with bulky molecules are suitable for contact angle measurements to characterize polymeric surfaces.

On the other hand, contact angles of a series of n-alkanes ranging from n-hexane to n-hexadecane on Teflon deviated somewhat from that curve. It was argued that these deviations result from a change in solid–liquid interfacial tensions, solid–vapor interfacial tensions, or both. In the case of short-chain n-alkanes, it appears that adsorption of vapor onto the solid changes γ_{sv}. On the other hand, it was argued that the reason for contact angle deviation of long-chain n-alkanes is a substrate-induced parallel reorientation of the liquid molecules at close vicinity of the solid. This in turn changes γ_{sl} and causes the deviations in contact angles from the smooth curve. In fact, parallel alignment of n-hexadecane molecules within the boundary regime to the solid surface is the reason for the superior nanolubricity of this liquid compared with OMCTS, which does not undergo significant molecular coordination at the solid–liquid interface [44]. It was concluded that because of the deviations in contact angles of n-alkanes from the smooth curve, the equation of state (Equation (6)) is not strictly applicable to their contact angles and only provides a good approximation to the solid surface tension.

The purpose of this article is to elucidate further the underlying reasons for deviations in contact angles from smooth curves. To that end, more liquids with bulky molecules were chosen for contact angle measurements on Teflon AF 1600 films in order to test whether or not the trend observed for such liquids in the previous study [43] is general. In addition, in light of the results obtained, criteria will be established for the determination of accurate solid surface tensions.

EXPERIMENTAL

Materials (Solid Surface and Liquids)

A 6% solution of Teflon® AF 1600 in Fluorinert® FC-75 (the solution is referred to as Teflon AF 1601S) purchased from Dupont Co. (Mississauga, ON, Canada) was selected as the coating material. Teflon AF 1600 is a copolymer of 35% TFE and 65% PDD (2,2-bistrifluoromethyl-4,5-difluoro-1,3-dioxole) with remarkable electrical, mechanical, and chemical characteristics [45, 46].

Silicon wafers ⟨100⟩ (Silicon Sense, Nashua, NH, USA; thickness: $525 \pm 50\,\mu\text{m}$) were selected as the substrate because of their smoothness, rigidity, and high surface tension. The latter property causes the polymeric coating solution to spread on the surfaces uniformly during the coating process [47]. The surfaces were coated by a dip-coating technique described as follows:

The substrates were cut into appropriate shapes from the original disks, and a hole of approximately 1 mm in diameter was drilled in the center of each surface. To clean the surfaces, chromic acid was spread on them and left for a short period of time. Then hydrogen peroxide (30% pure) was used to remove chromic acid by the resultant reaction. Finally the surfaces were rinsed with distilled water, ethanol, and isopropanol and were blown dry by nitrogen after each rinsing step. To enhance adhesion of the coating layer to the substrates and its stability, the cleaned surfaces were exposed to the vapor of an adhesion-promoting material, 1,1,1,3,3,3-Hexamethyldisilazane (HMDS) (Fluka, Oakville, ON, Canada; 99% pure), for 12 at 70°C.

In order to obtain smooth coating films, the 6% Teflon solution was diluted in the FC-75 solvent at a 1:1 volumetric ratio. The cleaned substrates were immersed vertically into the coating solution at a speed of 8×10^{-2} cm/s and withdrawn at the same speed. According to the supplier of Teflon AF 1600, freshly coated surfaces must be heated above the glass transition temperature of Teflon, T_g (160°C), to remove the solvent completely. This produces a smooth coating and improves adhesion of the polymer to the substrate [45]. Therefore, after the surfaces were coated with Teflon, they were kept inside an oven at 165°C for 24 h. Then the oven was turned off and the surfaces were cooled down gradually to ambient temperature.

This technique produces high-quality coated solid surfaces. The morphology of the polymeric surfaces was characterized by scanning force microscopy (SFM; NanoScope III, Digital Instruments, Santa Barbara, CA, USA) in the tapping mode. The Teflon films were very smooth, with RMS mean roughness of 0.3–0.4 nm (scan size: $20 \times 20\,\mu m^2$) and maximum peak-to-valley distances of about 2 nm, and they showed no additional structure.

The eleven liquids with bulky molecules chosen for this study are: p-xylene, o-xylene, 1-bromonaphthalene, lepidine, ethyl trans-cinnamate, 4- benzylisothiazole diethyl phthalate, 2-pyridyl carbinol, dibenzylamine, benzyl benzoate, and trans, trans, cis-1, 5, 9-cyclododecatriene. All liquids were purchased from Sigma-Aldrich Co. (Oakville, ON, Canada) at the highest purity available.

METHODS AND PROCEDURES

Axisymmetric Drop Shape Analysis-Profile (ADSA-P)

In principle, the shape of a drop is determined by the balance between gravity and interfacial tension. While gravity tends to flatten the sessile drop, interfacial tension tries to minimize the surface area and makes the drop spherical. The final shape of the drop is defined by the Laplace equation of capillarity.

The experimental drop profile is assumed to be axisymmetric and Laplacian. ADSA-P finds the theoretical drop profile that best matches the drop profile extracted from the image of a real drop. From the best match, ADSA-P determines not only contact angles but also volume and surface area of the drop, the three-phase contact radius, and the liquid–vapor interfacial tension. Details can be found elsewhere [48].

The contact angles reported in this article were determined by sessile drop experiments and were analyzed by ADSA-P. During the experiments, the ambient temperature and relative humidity were 23 ± 0.5°C and approximately 50%, respectively. A bubble level was first used to level the platform. A solid surface was carefully placed on the platform such that a stainless steel syringe needle passes through the hole in the center of the surface. To prevent leakage of liquid between the needle and the hole, Teflon tape was wrapped around the needle before insertion into the hole. The needle was positioned such that its tip was just above the solid surface. To ensure that the advancing drop grows axisymmetrically in the center of the image field and does not hinge on the lip of the hole, an initial drop of a few millimeters was deposited from above to cover the 1 mm diameter hole on the surface. A motorized syringe was then operated at a constant speed. Liquid was supplied steadily into the drop so that low-rate advancing contact angles were obtained. The images of the drop were recorded during the experiment and analyzed by ADSA-P afterwards.

Figure 3 shows a typical output of ADSA-P obtained from a contact angle experiment with o-xylene on Teflon (corresponding to run number 6 in Table 1). Several traces were obtained as a function of time, *i.e.*, contact angle, θ; three-phase contact radius, R; drop volume, V; and liquid–vapor interfacial tension, γ_{lv}.

RESULTS AND DISCUSSION

In order to find out whether the contact angle of any liquid with bulky molecules would follow the pattern observed for the five liquids with bulky molecules studied before, more liquids of this type (as listed above) were chosen for advancing contact angle measurements. To ensure the reproducibility of the contact angles, measurements were performed at least five times for each liquid, each on a freshly prepared solid surface. As an example, contact angles of o-xylene obtained in six different experiments are given in Table 1. Since contact angles were constant during these experiments, they were averaged and yielded a mean contact angle of o-xylene on Teflon of 71.17 ± 0.13 degrees.

Table 2 summarizes contact angles of the sixteen liquids with bulky molecules (five liquids from the previous study and 11 new liquids). The contact angles in this table are the average of values, obtained just as for o-xylene. The surface tension value of each liquid, γ_{lv}, represented in the table was measured separately in pendant drop experiments [48].

Figure 4 illustrates the plot of $\gamma_{\mathrm{lv}} \cos\theta$ *versus* γ_{lv} for all of the liquids with bulky molecules, *i.e.*, both from the previous and the current study. In this figure, three different symbols are used to represent the contact angle data. The round symbols correspond to the five liquids used before, the squares represent those liquids used in this study that fall on the same curve, and the triangles show the liquids whose contact angles deviate from this curve. While contact angles of ten liquids fall perfectly on a curve corresponding to $\beta = 0.0001161\ (\mathrm{mJ/m^2})^{-2}$ and $\gamma_{\mathrm{sv}} = 13.61\,\mathrm{mJ/m^2}$, as determined by the multivariable optimization scheme, six liquids show small deviations from this curve, up to approximately three degrees. In order to

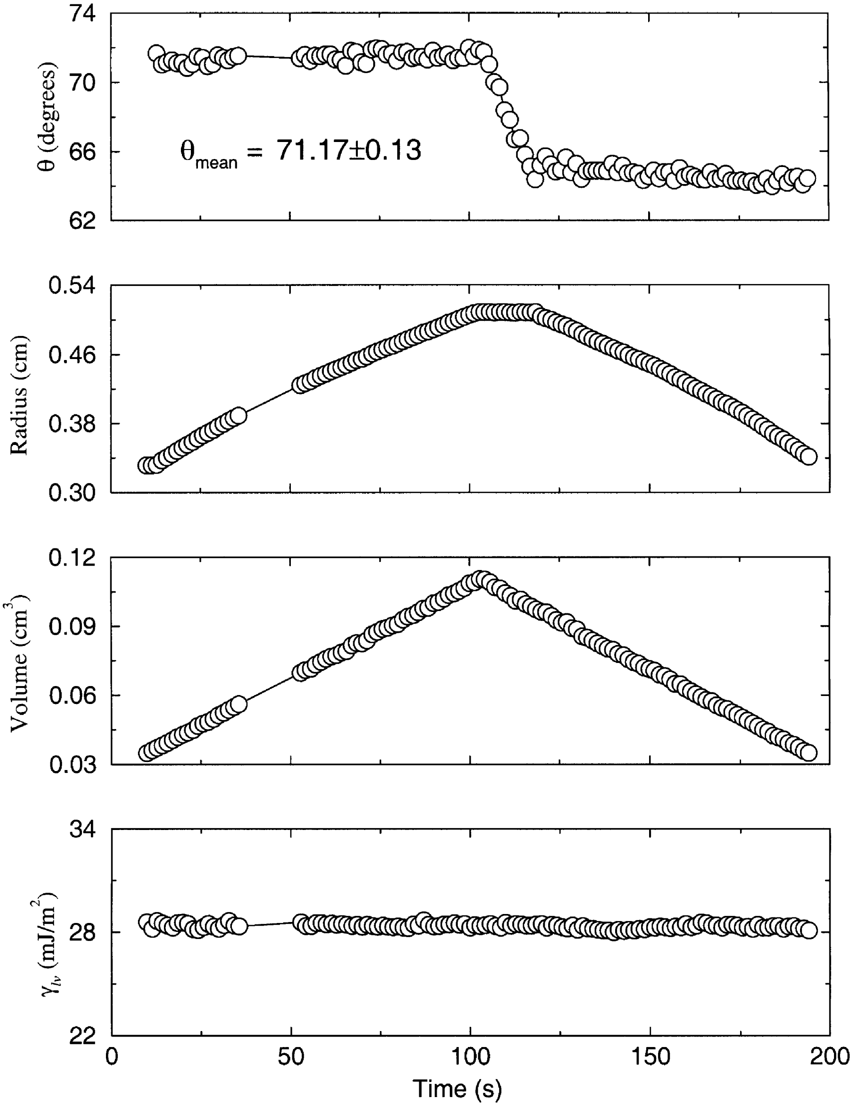

FIGURE 3 A typical output of ADSA-P for a sessile drop experiment of o-xylene on a Teflon®-coated silicon wafer giving contact angle, the three-phase contact radius, drop volume, and the liquid–vapor interfacial tension. These curves correspond to run number 6 in Table 1.

TABLE 1 Advancing Contact Angles of o-xylene on Teflon® Films from Six Different Sessile Drop Experiments, Each on a New Film. The 95% confidence limits of the measurements are also given.

Run number	Advancing contact angle, θ (degrees)	95% confidence limits
1	71.07	0.13
2	71.32	0.14
3	71.10	0.09
4	71.03	0.12
5	71.30	0.16
6	71.22	0.22
	Mean 71.17 ± 0.13 degrees	

explain the observed patterns for these liquids, they are divided into two groups as follows:

Liquids with Bulky Molecules, First Group

This group includes the liquids represented by round and square symbols in Figure 4. It can be seen that the contact angles of these liquids fall very well on the smooth curve of $\gamma_{sv} = 13.61\,\mathrm{mJ/m^2}$. Table 3 lists

TABLE 2 Summary of Liquid Surface Tension, Contact Angle, and Vapor Pressures of 16 Liquids with Bulky Molecules

Liquid	γ_{lv} (mJ/m^2)	θ (degree)	p_v (psi)
OMTS	16.72	35.75 ± 0.12	0.0502
OMCTS	18.20	43.68 ± 0.13	0.0157
P-Xylene	27.90	68.65 ± 0.09	0.1721
O-Xylene	29.30	71.17 ± 0.13	0.1282
Cis-decalin	32.16	75.53 ± 0.22	0.0132
Trans,trans,cis-1,5,9-cyclododecatriene	33.88	78.29 ± 0.19	0.0004
Tetralin	36.15	81.06 ± 0.20	0.0061
Ethyl trans-cinnamate	36.60	84.68 ± 0.14	0.0054
Diethylphthalate	36.67	84.73 ± 0.27	0.000009
Methyl salicylate	38.71	83.69 ± 0.23	0.0005
Dibenzylamine	39.70	88.25 ± 0.29	0.0105
Benzyl benzoate	41.75	89.20 ± 0.19	0.0193
Lepidine	43.20	89.49 ± 0.65	0.00018
1-Bromonaphthalene	43.70	89.80 ± 0.44	0.00019
4-Benzylisothiazole	44.03	92.46 ± 0.36	—
2-Pyridyl carbinol	47.55	96.70 ± 0.11	—

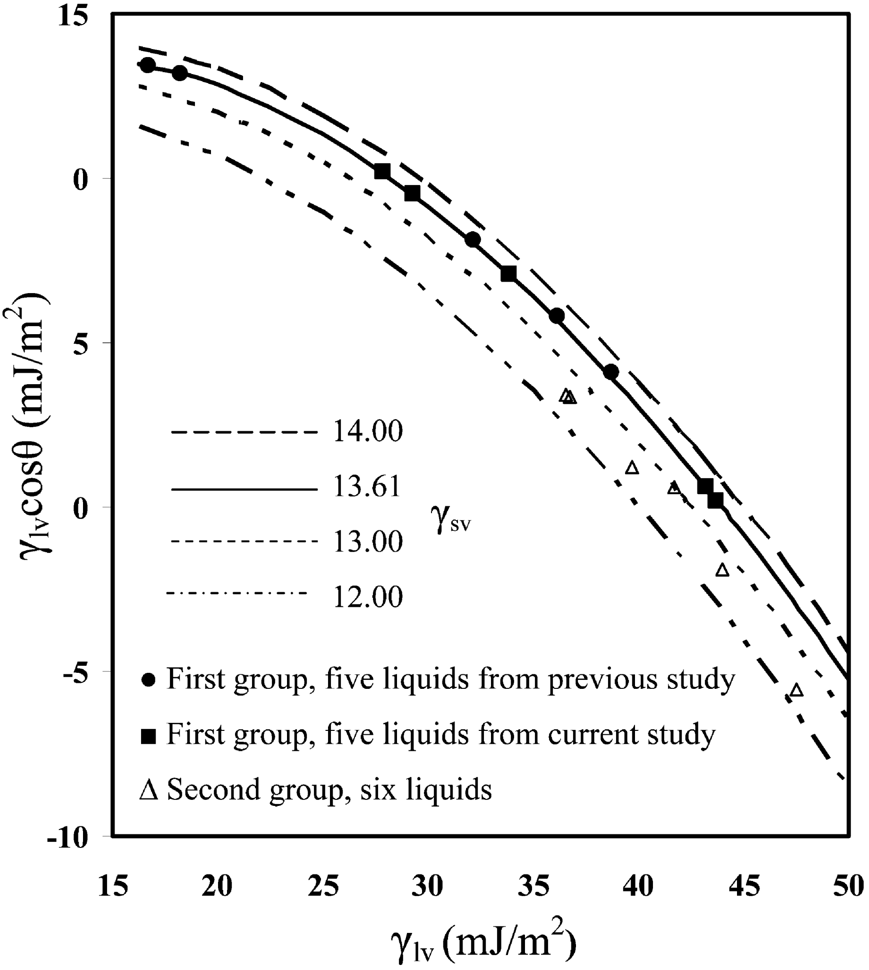

FIGURE 4 Plot of $\gamma_{lv}\cos\theta$ *versus* γ_{lv} for liquids with bulky molecules. The first group includes 10 liquids described by round or rectangular symbols. The 6 liquids in the second group are represented by triangular symbols.

the contact angle deviation, $\Delta\theta$, for each of these liquids from this curve. The minus sign for deviations means that the experimental contact angle is above the curve, while the plus sign shows that the contact angle falls below the curve. The deviations are indeed small, averaging only ± 0.24 degrees. This translates into $\pm 0.07\,\mathrm{mJ/m^2}$ in the γ_{sv} value. Among these liquids, only OMTS shows a fairly large deviation with -0.89 degrees. This could be due to the nonlinearity of the cosine function.

TABLE 3 Contact Angle Deviations of the First Group of Liquids with Bulky Molecules from the Smooth Curve of $\gamma_{sv} = 13.61\,mJ/m^2$. The solid surface tension values obtained from the two different β values (*cf.* text) are also illustrated.

Liquid	$\Delta\theta$ (degrees)	γ_{sv} (mJ/m^2) ($\beta = 0.0001161$)	γ_{sv} (mJ/m^2) ($\beta = 0.0001135$)
OMTS	− 0.89	13.75	13.74
OMCTS	+ 0.17	13.58	13.58
P-Xylene	0.00	13.61	13.60
O-Xylene	+ 0.12	13.57	13.56
Cis-decalin	+ 0.01	13.61	13.58
Trans,trans,cis-1,5,9-cyclododecatriene	+ 0.33	13.50	13.47
Tetralin	+ 0.09	13.58	13.55
Methyl salicylate	− 0.44	13.77	13.73
Lepidine	+ 0.30	13.49	13.45
1-Bromonaphthalene	+ 0.07	13.58	13.53
Mean	± 0.24°	13.59 ± 0.07 (mJ/m^2)	13.58 ± 0.10 (mJ/m^2)

An interesting result is the consistency of the previously obtained γ_{sv} and β values and their new values. From the earlier contact angles of the five liquids, represented by round symbols in Figure 4, we obtained the values of $\beta = 0.0001135$ $(mJ/m^2)^{-2}$ and $\gamma_{sv} = 13.64$ mJ/m^2 [43]. This γ_{sv} is essentially identical to its new value, *i.e.*, $\gamma_{sv} = 13.61\,mJ/m^2$, obtained here. Furthermore, the two β values are also in a good agreement. This is shown in Table 3 by presenting two sets of γ_{sv} values. These γ_{sv} values were calculated from Equation (6) using each pair of γ_{lv} and θ for the first group of liquids with bulky molecules and the two β values. It can be seen that each pair of γ_{sv} values for a given liquid and also the average value from each column are essentially the same. This indicates that such small differences in β values do not affect γ_{sv} values significantly. The same conclusion can be drawn using $\beta = 0.0001247$ $(mJ/m^2)^{-2}$ obtained before [41] and either of the β values presented above.

The results suggest that the 10 liquids in this group do not interact with the Teflon films in a specific fashion. This is plausible because the bulky molecules are larger than the mean roughness of the solid, so that they do not fit into the morphological patterns of the solid surface. Therefore, the solid surface cannot restructure them significantly at the solid−liquid interface, and hence $\gamma_{sl,}$ remains unchanged. Knowing that the solid-vapor interfacial tension, γ_{sv}, is also constant because of the extremely low vapor pressure of these liquids, it appears that liquids with bulky molecules are suitable for characterizing the energetics of polymeric surfaces using the equation of state approach.

Liquids with Bulky Molecules, Second Group

The plot of Figure 4 shows that contact angles of 10 liquids with bulky molecules (first group) fall perfectly on a smooth curve that is believed to represent the exact surface tension of the Teflon film, *i.e.*, $\gamma_{sv} = 13.61 \pm 0.07\,mJ/m^2$. If size and shape of molecules of a liquid were the only parameters affecting the contact angle of a solid–liquid system, then contact angles of all 16 liquids would fall perfectly on the curve in Figure 4. However, this is not the case. The contact angles of a second group of liquids with fairly bulky molecules represented by triangular symbols shows some deviation. Table 4 gives this deviation in contact angle for each of these liquids. It is seen that the deviations can be up to ~3 degrees. Since the molecules of these liquids possess similar geometrical characteristics to the first group in terms of shape and size, it is postulated that there must be additional factors affecting contact angle and surface tension values.

Since it is assumed that both γ_{lv} and θ are correctly measured quantities, only a change in γ_{sv} and/or γ_{sl} can cause the contact angle deviations. Because of the extremely low vapor pressure of these liquids (shown in Table 2), adsorption of their vapor onto the solid surface is unlikely to contribute to contact angle deviations, and the reason must be sought in the solid–liquid interfacial tension.

The main difference between the two groups of liquids lies in their chemical structure. Figure 5 shows the molecular structure of both groups of liquids with bulky molecules generated using CORINA [49, 50], which is a three-dimensional (3D) structure generator software. It is seen that unlike most of the liquids in the first group

TABLE 4 Contact Angle Deviations of the Second Group of Liquids with Bulky Molecules from the Smooth Curve of $\gamma_{sv} = 13.61\,mJ/m^2$

Liquid	$\Delta\theta$ (degrees)
Ethyl trans-cinnamate	+3.13
Diethyl phthalate	+3.09
Dibensylamine	+2.96
Benzyl benzoate	+1.58
4-Bensylisothiazole	+2.54
2-Pyridyl carbinol	+3.03

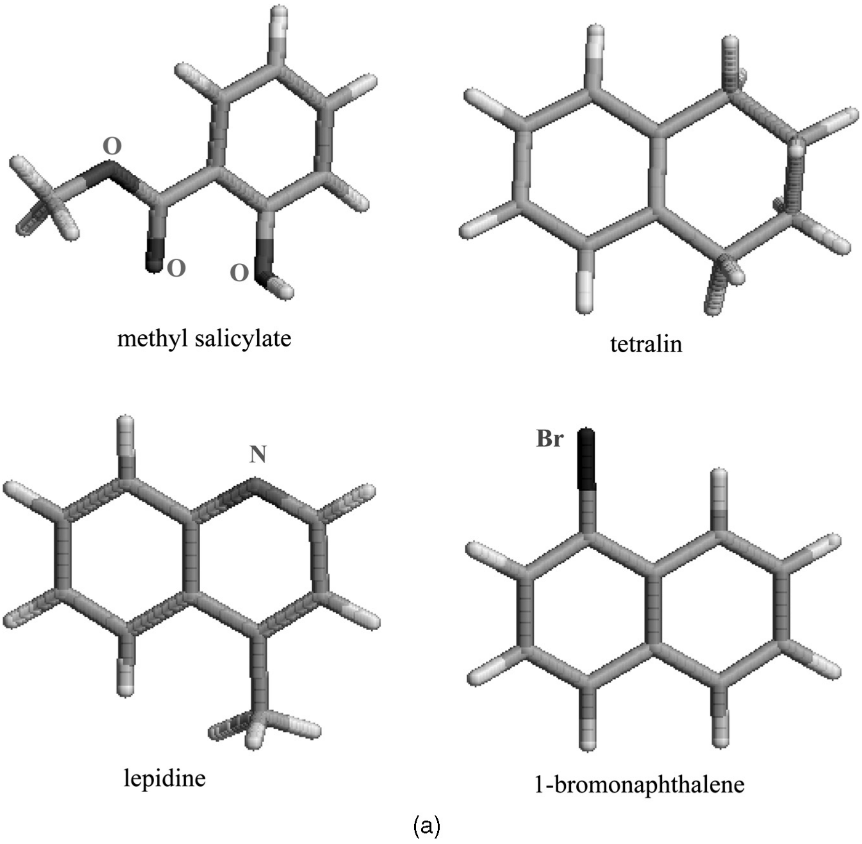

methyl salicylate

tetralin

lepidine

1-bromonaphthalene

FIGURE 5 Molecular structures of both groups of liquids with bulky molecules generated by the CORINA software. The first group is shown in Figure 5a and the second group in Figure 5b, respectively. The main difference between the two groups is the presence of the electronegative oxygen and nitrogen atoms in the molecules of the second group. (*Continued*).

(see Figure 5a), all liquid molecules in the second group (Figure 5b) contain nitrogen atoms (N), oxygen atoms (O), or both. These two atoms are known to be highly electronegative, and their presence in a molecule causes a nonuniform electron density distribution over the molecule. As a result, the part of the molecule including these atoms becomes more negatively charged. This is also true for the solid phase. Teflon AF 1600 is a very hydrophobic copolymer. The reason for its very low surface energy is the existence of CF_2 and CF_3 moieties in the polymeric chains (A detailed analysis of the chemical surface

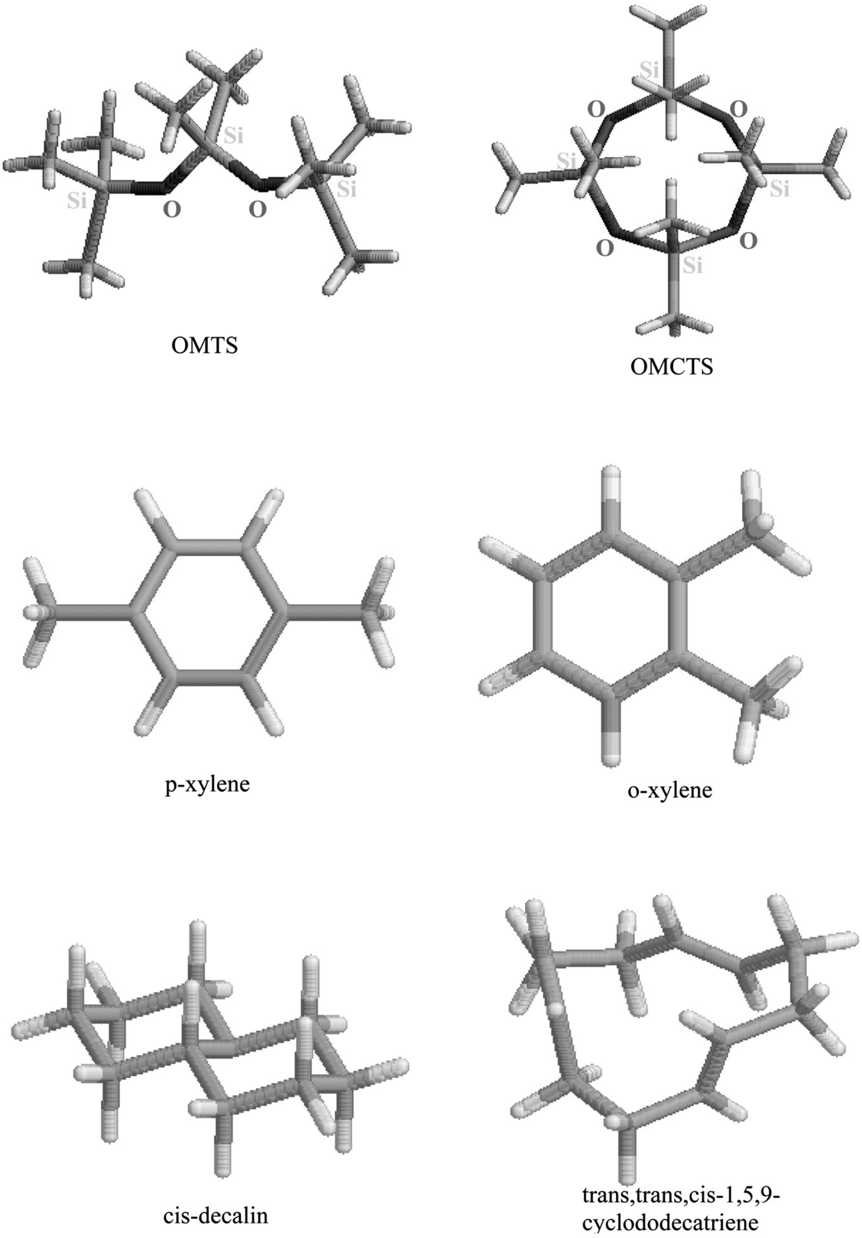

OMTS

OMCTS

p-xylene

o-xylene

cis-decalin

trans,trans,cis-1,5,9-cyclododecatriene

(a) continued

FIGURE 5 (Continued).

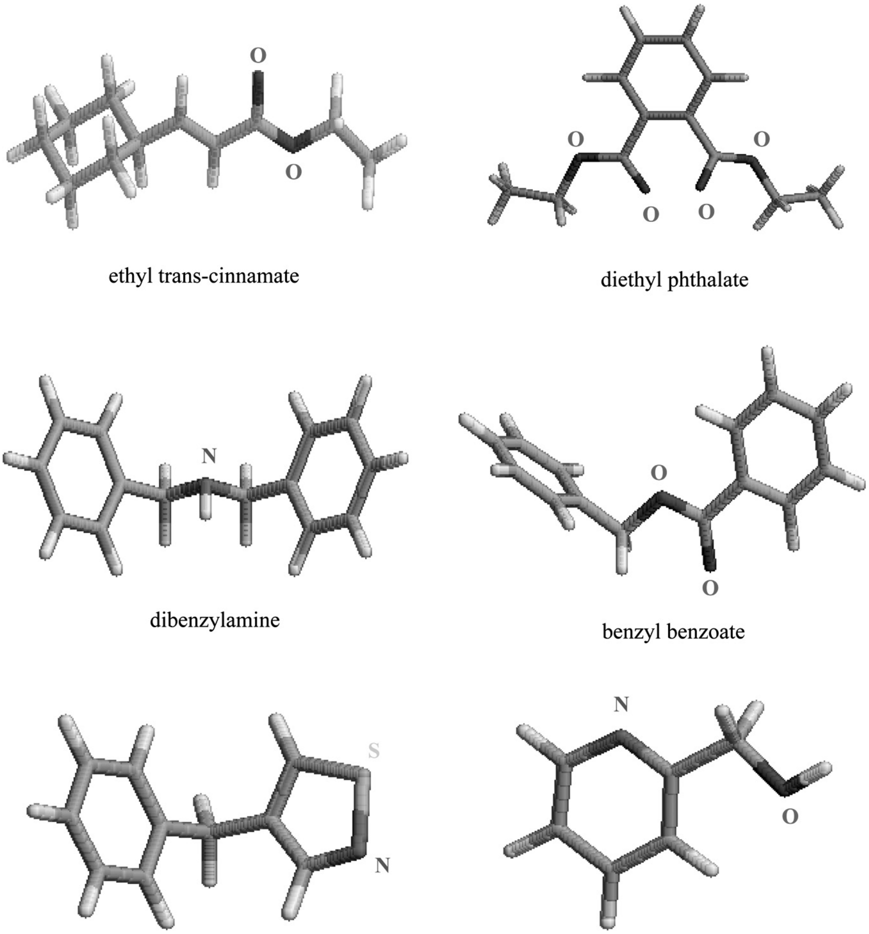

ethyl trans-cinnamate

diethyl phthalate

dibenzylamine

benzyl benzoate

4-benzylisothiazole

2-pyridyl carbinol

(b)

FIGURE 5 (Continued).

composition (XPS spectrum) of Teflon AF1600, including its structure formula, can be found in Sacher and Klemberg-Sapieha [51]). Since fluorine has the highest electron affinity known, the electron density will be higher around the fluorine-containing part of the solid molecules. It is speculated that when liquid molecules approach a Teflon surface, since like charges repel each other the negatively charged parts of the liquid molecules are repelled by the solid molecules, whose fluorine atoms are directed outward. This causes liquid molecules to be reoriented at the solid–liquid interface with their negatively charged sides directed away from the solid. Such a change in conformations of liquid molecules at the solid–liquid interface yields a consequent change in the corresponding interfacial tension, γ_{sl}, and would explain the deviation in the contact angles from the smooth curve of $\gamma_{sv} = 13.61\,\mathrm{mJ/m^2}$.

It might be argued that reorientation could take place for the solid-phase molecules rather than for the liquid molecules. This is because polymeric chains are known to be mobile and can be restructured in response to the change in environment (from air to liquid) by disappearance of hydrophobic CF_2 and CF_3 groups from the top layer of the solid surface [52–55]. However, migration of these moieties into the bulk solid phase makes the solid surface more hydrophilic. This would yield a lower contact angle for the liquids in the second group and would cause the experimental points to fall above the curve of $\gamma_{sv} = 13.61\,\mathrm{mJ/m^2}$. Therefore, change in surface configuration of the Teflon films cannot be the reason for contact angle deviations of these liquids, although this phenomenon is believed to be manifested in contact angle hysteresis.

For the liquids that contain a hydrogen-bonding moiety in their molecular structure, *i.e.*, dibenzylamine and 2-pyridyl carbinol, a second possibility exists as well. Because of the higher electronegativity of fluorine atoms compared with oxygen and nitrogen atoms, the H-bonding hydrogen from the liquid molecules is attracted to the fluorine atom of the Teflon molecule and forms a new H-bond with it. The formation of this new bond (F—H) is favorable since it is an energy-releasing interaction whose energy is higher than the dissociation energy of O—H and N—H bonds. Such interactions change the properties of solid and liquid molecules at the solid–liquid interface from the corresponding bulk phases. This in turn causes a change in γ_{sl} so that the measured contact angle is a representative value of the changed energetics and, therefore, will deviate from the $\gamma_{sv} = 13.61\,\mathrm{mJ/m^2}$ curve. Formation of H-bonds between solid and liquid molecules upon their contact has been reported in the literature [56]. It should be noted, however, that the two hydrogen-bond–forming liquids, *i.e.*, dibenzylamine and 2-pyridyl carbinol, do not produce results outside the range of the nonhydrogen-bonding bulky molecules containing O or N atoms.

One might argue that if the presence of oxygen and nitrogen atoms indeed causes the deviations in contact angles of liquids in the second group from the smooth curve of $\gamma_{sv} = 13.61\,\mathrm{mJ/m^2}$, the contact angle of lepidine, which contains nitrogen atoms, from the first group should also deviate from this curve. The fact that it does not may possibly be due to the fact that ADSA-P is not very accurate when contact angle is near 90 degrees and the corresponding 95% confidence limit is high (0.65 degrees in this case). However, since the mean value fell on this curve, the result was included in the first group of liquids with bulky molecules.

It is also to be noted that the contact angle of n-hexadecane, which is a totally dispersive liquid, showed a deviation of ~ 2 degrees from the $\gamma_{sv} = 13.61\,\mathrm{mJ/m^2}$ curve [43]. This is in the range of deviations of the liquids with bulky molecules containing N atoms, O atoms, or both. It is concluded that steric properties can play a role just as significant as intermolecular forces.

Further insight into how all such phenomena contribute to contact angle deviations could be gained by studying conformations of liquid molecules when exposed to the solid surface, *e.g.*, by molecular dynamics.

CRITERIA FOR THE DETERMINATION OF ACCURATE SOLID SURFACE TENSIONS

With respect to the determination of solid surface tension from contact angles, the following picture emerges. In the case of the first group of liquids with bulky molecules that do not undergo specific interactions with Teflon, the equation of state (Equation (6)) provides the exact surface tension of the solid. However, n-alkanes and the second group of liquids with bulky molecules showed specific interactions with Teflon that were excluded by the assumptions made in deriving Equation (5) [41]. Since γ_{sl} is presumably not a precise function of γ_{lv} and γ_{sv} in these cases, the equation of state is not strictly applicable to their contact angles and provides only a good approximation for the solid surface tension.

According to the results obtained so far, at least the following conditions should be met, though there might be other factors as-yet unknown:

1. The liquid molecules should be bulky. This decreases the number of possible interacting sites on the solid surface. Any chain-like molecule could cause specific interactions determined by the molecular structure of solid and liquid.
2. The liquids should not have the propensity for electronegative moieties in the molecule to cause specific attraction, repulsion, or ordering.
3. The liquids should have low vapor pressure to eliminate or reduce vapor adsorption. Fortunately, the vapor pressure of most liquids with bulky molecules is very low.

4. The solid surface should be as smooth as possible, with mean roughness well below 0.5 nm, so that the liquid molecules do not fit into morphological features on the solid.
5. The liquid should be chemically inert.

If these conditions are met, solid surface tension values may be obtainable with an accuracy of $\pm 0.1\,\mathrm{mJ/m^2}$.

SUMMARY

A further investigation of the reasons for deviations in contact angles of liquids from smooth curves is presented. It was shown that contact angles of a first group of liquids with bulky molecules fall perfectly on a smooth curve of $\gamma_{\mathrm{sv}} = 13.61 \pm 0.07\,\mathrm{mJ/m^2}$, which is believed to be the exact surface tension of Teflon AF 1600. This was due to the fact that these liquids have both extremely low vapor pressure and do not interact in a specific way with Teflon films. Therefore, the interfacial tensions follow an ideal pattern. However, a second group of liquids with bulky molecules showed small deviations from this curve because of specific interactions with the solid surface, causing the solid–liquid interfacial tensions to deviate from the ideal pattern. Because of the deviations in contact angles of these liquids, the equation of state is not strictly applicable and only provides a good approximation to the energetics of the solid surface. Criteria were also established for determination of accurate solid surface tensions from contact angles.

REFERENCES

[1] Zisman, W. A., Contact angle, wettability and adhesion, In: *Advances in Chemistry*, F. M. Fowkes, Ed. (American Chemical Society, Washington, DC, 1964), Vol. 43.
[2] Fowkes, F. M., *Ind. Eng. Chem.* **12**, 40–52 (1964).
[3] Driedger, O., Neumann, A. W., and Sell, P. J., *Kolloid-Z. Z. Polym.* **201**, 52–57 (1965).
[4] Spelt, J. K. and Li, D., In: *Applied Surface Thermodynamics*, 1st ed., A. W. Neumann and J. K. Spelt, Eds. (Dekker, New York, 1996), Chap. 5, pp. 239–292.
[5] Owens, D. K. and Wendt, R. C., *J. Appl. Polym. Sci.* **13**, 1741–1747 (1969).
[6] van Oss, C. J., Chaudhury, M. K., and Good, R., *J. Chem. Revs.* **88**, 927–941 (1988).
[7] Good, R. J. and van Oss, C. J., In: *Modern Approaches to Wettability: Theory and Applications*, M. Schrader and G. Loeb, Eds. (Plenum Press, New York, 1992), pp. 1–27.
[8] Derjaguin, B. V., Muller, V. M., and Toporov, Y. P., *J. Colloid Interface Sci.* **73**, 293–293 (1980).
[9] Johnson, K. L., Kendall, K., and Roberts, A. D., *Proc. R. Soc. London* **A324**, 301–313 (1971).
[10] Fogden, A. and White, L. R., *J. Colloid Interface Sci.* **138**, 414–430 (1990).
[11] Christenson, H. K., *J. Phys. Chem.* **90**, 4–6 (1986).

[12] Claesson, P. M., Blom, C. E., Horn, P. C., and Ninham, B. W., *J. Colloid Interface Sci.* **114**, 234–242 (1986).

[13] Pashley, P. M., McGuiggan, P. M., and Pashley, R. M., *Colloids Surf.* **27**, 277–287 (1987).

[14] Pashley, R. M., McGuiggan, P. M., Ninham, B. W., and Evans, D. F., *Science* **229**, 1088–1089 (1985).

[15] Omenyi, S. N. and Neumann, A. W., *J. Appl. Phys.* **47**, 3956–3962 (1976).

[16] Li, D. and Neumann, A. W., In: *Applied Surface Thermodynamics*, 1st ed., A. W. Neumann and J. K. Spelt, Eds. (Dekker, New York, 1996), Chap. 12, pp. 557–628.

[17] Corte, A. E., *J. Geophys. Res.* **67**, 1085–1090 (1962).

[18] Hoekstra, P. and Miller, R. D., *J. Colloid Interface Sci.* **25**, 166–173 (1967).

[19] Cissé, J. and Bolling, G. F., *J. Crystal Growth* **10**, 67–76 (1971).

[20] Cissé, J. and Bolling, G. F., *J. Crystal Growth* **11**, 25–28 (1971).

[21] Chen, K. H. and Wilcox, W. R., *J. Crystal Growth* **40**, 214–220 (1977).

[22] Fuerstenau, D. W. and Williams, M. C., *Colloids Surf.* **22**, 87–91 (1987).

[23] Fuerstenau, D. W. and Williams, M. C., *Part. Charac.* **4**, 7–13 (1987).

[24] Fuerstenau, D. W. and Williams, M. C., *J. Mineral Process* **20**, 153–157 (1987).

[25] Fuerstenau, D. W., Diao, J., and Hanson, J., *Energy Fuels* **4**, 34–37 (1990).

[26] Grundke, K., Bogumil, T., Gietzelt, T., Jacobasch, J.-H., and Neumann, A. W., *Prog. Colloid Polym. Sci.* **101**, 58–68 (1996).

[27] Vargha-Butler, E. I., Moy, E., and Neumann, A. W., *Colloids Surf.* **24**, 315–324 (1987).

[28] Vargha-Butler, E. I., Zubovits, T. K., Absolom, D. R., and Neumann, A. W., *Chem. Eng. Commun.* **33**, 255–276 (1985).

[29] Li, D. and Neumann, A. W., *Applied Surface Thermodynamics*, 1st ed., A. W. Neumann and J. K. Spelt, Eds. (Dekker, New York, 1996), Chap. 11, pp. 509–556.

[30] Hemingway, S. J., Henderson, J. R., and Rowlinson, J. R., *Faraday Symp. Chem. Soc.* **16**, 33–43 (1981).

[31] Guermeur, R., Biquard, F., and Jacolin, C., *J. Chem. Phys.* **82**, 2040–2051 (1985).

[32] Moy, E. and Neumann, A. W., In: *Applied Surface Thermodynamics*, 1st ed., A. W. Neumann and J. K. Spelt, Eds. (Dekker, New York, 1996), Chap. 7, pp. 333–378.

[33] Hamaker, H. C., *Physica* **4**, 1058–1072 (1937).

[34] Israelachvili, J. N., *Proc. R. Soc. London* **A331**, 39–55 (1972).

[35] van Giessen, A. E., Bukman, D. J., and Widom, B., *J. Colloid Interface Sci.* **192**, 257–265 (1997).

[36] Reed, T. M., *J. Phys. Chem.* **59**, 425–428 (1955).

[37] Fender, B. E. F. and Halsey, G. D., Jr., *J. Chem. Phys.* **36**, 1881–1888 (1962).

[38] Sullivan, D. E., *J. Chem. Phys.* **74**, 2604–2615 (1981).

[39] Matyushov, D. V. and Schmid, R., *J. Chem. Phys.* **104**, 8627–8638 (1996).

[40] Young, T., *Philos. Trans. R. Soc. London* **95**, 65–87 (1805).

[41] Kwok, D. Y. and Neumann, A. W., *Adv. Colloid Interface Sci.* **81**, 167–249 (1999).

[42] Li, D. and Neumann, A. W., *J. Colloid Interface Sci.* **148**, 190–200 (1992).

[43] Tavana, H., Lam, C. N. C., Grundke, K., Friedel, P., Kwok, D. Y., Hair, M. L., and Neumann, A. W. Contact angle measurements with liquids consisting of bulky molecules, Accepted. *J. Colloid Int. Sci.*

[44] He, M., Blum, A. S., Overney, G., and Overney, R., *Phys. Rev. Lett.* **88**, 1–4 (2002).

[45] DuPont Inc., Product information: Teflon AF Amorphous Fluoropolymers, (2/98) (Wilmington, 1998) 204103D.

[46] Buck, W. H., and Resnick, P. R., Teflon AF amorphous fluoropolymers technical information: Properties of amorphous fluoropolymers based on 2, 2-bistrifluoromethyl-

4, 5-difluoro-1, 3-dioxole, *Paper Presented at the 183rd Meeting of the Electrochemical Society*, Honolulu, HI, 17 May 1993.

[47] Lam, C. N. C., Wu, R., Li, D., Hair, M. L., and Neumann, A. W., *Adv. Colloid Interface Sci.* **96**, 169–191 (2002).

[48] Lahooti, S., Del Rio, O. I., Cheng, P., and Neumann, A. W., In: *Applied Surface Thermodynamics*, 1st ed., A. W. Neumann and J. K. Spelt, Eds. (Dekker, New York, 1996), Chap. 10, pp. 441–507.

[49] Sadowski, J. and Gasteiger, J., *Chem. Rev.* **93**, 2567–2581 (1993).

[50] Sadowski, J., Gasteiger, J., and Klebe, G., *J. Chem. Inf. Comput. Sci.* **34**, 1000–1008 (1994).

[51] Sacher, E. and Klemberg-Sapieha, J. E., *J. Vac. Sci. Technol. A.* **15**, 2143–2147 (1997).

[52] Yasuda, T., Okuno, T., and Yoshida, K., *J. Polym. Sci. B: Polym. Phys.*, **26**, 1781–1794 (1988).

[53] Yasuda, T., Miyama, M., and Yasuda, H., *Langmuir*, **8**, 1425–1430 (1992).

[54] Wang, J.-H., Claesson, J. L., and Yasuda, H., *Langmuir*, **10**, 3887–3897 (1994).

[55] Cross, E. M. and McCarthy, T. J., *Mocromolecules*, **23**, 3916–3922 (1990).

[56] Lee, S. H. and Rossky, P. J., *J. Chem. Phys.* **100**, 3334–3345 (1994).